XLI CILAMCE
XLI Ibero-Latin American Congress on Computational Methods in Engineering
16-19 November, 2020 FOZ DO IGUAÇU PARANÁ - BRAZIL

Flutter analysis of a tip-mass-wing using Rayleigh-Ritz by hierarchical polynomials

Thais Cardoso Franco[1], Flávio Luiz Cardoso Ribeiro[1]

[1]*Aeronautics Institute of Technology (ITA)*
Praça Marechal Eduardo Gomes, 50 - São José dos Campos, Brazil
thais17franco@gmail.com, flaviocr@ita.br

Abstract. In an attempt to reduce fuel consumption and noise, aircraft designers try to minimize structural weight and maximize the wing aspect ratio. Both constraints lead to an increase in structural flexibility. Consequently, aeroelastic effects, as flutter, must be researched extensively from conceptual design stages. In order to avoid flutter, several studies have been conducted seeking to use active control techniques using piezoelectric materials. This paper proposes to analyze the vibration frequencies and flutter velocities of a wing model described as a clamped-free beam with bending and torsion movements with mass at its tip. A second model, the Goland wing, whose flutter speeds are widely reported in the literature, is used to validate the results of flutter velocity obtained for the propose model. To compare the accuracy of the results obtained and the computational cost, approximate methods are used to obtain the discrete structural equations: Rayleigh-Ritz with hierarchical standard and Bardell polynomials. The complete aeroelastic model is developed applying the Peters aerodynamic model, which approximates the effects of the unsteady incompressible flow using a state-space approximation. Thanks to the use of hierarchical polynomials, a low-order and computationally cheap numerical model is obtained. This model can be used for optimization in conceptual design stages, as well for feedback control design.

Keywords: flutter, aeroelastic analysis, unsteady theory, Hierarchical Rayleigh-Ritz.

1 Introduction

The reduction in fuel consumption, and the consequent reduction in the emission of pollutants and operating costs, can be achieved by optimizing the aircraft structure by reducing aerodynamic drag and its empty weight. Both strategies lead to elongated and flexible wings, making flexible aircraft objects of study more and more recurrent. Since aeroelastic phenomena can lead to structural failure, their effects have a major influence on the design and flight performance of new aircraft. The most studied effect of induced vibration is flutter. This instability involves two or more vibration modes and results from the unfavorable coupling of aerodynamic, inertial and elastic forces, which means that the structure can extract energy from the air flow. Among the difficulties in modeling the flutter phenomenon are the unsteady nature of the aerodynamic forces and the moments generated when the aircraft oscillates as described by Wright and Cooper [1]. The presence of flexible effects influences the dynamic stability modes of the rigid aircraft and therefore affects flight dynamics. The flutter can take various forms involving different pairs of interaction modes, the most studied of which are: bending and twisting of the wing, twisting of the wing and the control surface, coupling of the wing and motor modes.

During flutter, aerodynamic forces drive natural frequencies in their modes, especially the first two, usually associated with twisting and bending, to converge close to the critical flutter speed, detailing in Dowell et al. [2], Hodges and Pierce [3]. Above this speed, the amplitude of oscillations increases with time, until the deflections are large enough to cause a structural failure or create a permanent cycle. Below this speed, oscillations are attenuated; while above it, the energy from the fluid flow is transferred to the structure, generating increasing oscillations due to the displacement of one of the poles of the system to the unstable region, making it negatively damped.

In order to avoid flutter and increase the flight envelope of aircraft, several studies have been carried out seeking to use active control techniques. The use of piezoelectric materials as actuators is a possibility. In this context, this work aims to develop a semi-analytical tool that can be used for aeroelastic modeling of different structures with coupled piezoelectric material. Thanks to the low computational cost, the tool can be used for control system design, simulation, parametric studies and project optimization.

The objective of this work is to obtain a semi-analytical structural model that describes the aeroelastic problem, considering a bending and twisting beam, which is coupled with a piezoelectric element, which will later be used for structural control. To determine the behavior of the treated aeroelastic system, the unsteady aerodynamic model is used via the Peters method. To perform the discretization of the wing model, the approximate Rayleigh-Ritz methods via Bardell and Standard hierarchical polynomials are implemented from routines created in the MATLAB® environment. The use of global polynomials in the discretization allows to obtain models of reduced order in comparison with the Finite Elements, thus decreasing the computational cost.

Finally, it is important to note that this paper is a continuation of works already done by the authors in Franco [4], Franco and Cardoso-Ribeiro [5] of active control using piezoelectric elements. The novelty of this paper with respect to Franco and Cardoso-Ribeiro [5] is that we use Peter's method to represent unsteady aerodynamics.

This paper is divided as follows. Firstly, a description of the experimental device that is considered in this paper is presented in Section 2. Then, the unsteady aerodynamic model is shown in Section 3. The aeroelastic equations are derived in Section 4 and the approximation functions used are described in Section 5. Numerical results and a discussion is presented in Section 6. Finally, conclusions and further work are presented in Section 7.

2 Structure Materials and Dimensions

An experimental device depicted in Fig. 1 is considered, which consists of a flexible beam with a tip mass and a piezoelectric material, used to excite and to actively control the coupled system, reducing the vibrations. The values of properties for the beam and for the piezoelectric element can be found in Table 1. The simulations consist of a flight at sea level (ρ_f = 1.225 kg/m^3). The parameters p_1, p_2, p_3 and p_4 are such that it is possible to position the piezoelectric element centered on the beam along the chord (z direction) and the wingspan (x direction).

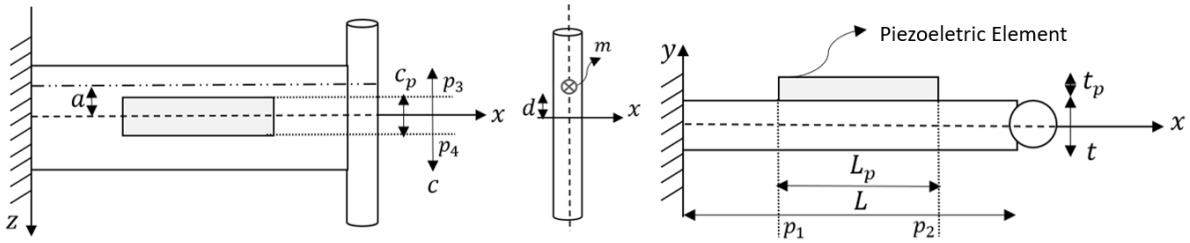

Figure 1. Schematic drawing of the beam with a piezoelectric element attached.

Table 1. Parameters

Wing Parameters	Value	Unity	Piezo Parameters	Value	Unity
Length L	0.35	m	Length L_p	0.14	m
Thickness t	0.000813	m	Thickness t_p	0.0001	m
Width $c = 2b$	0.04	m	Width c_p	0.035	m
Density ρ	2697	kg/m^3	Density ρ_p	2970	kg/m^3
Young modulus E	73.1	GPa	Young modulus E_p	67	GPa
Shear modulus G	28	GPa	Shear modulus G_p	28	GPa
Elastic axis location a	m	0			
Coupled mass m	kg	0.03458			
Offset d	mm	5			
Coupled mass inertia I_m	kg.m^2	1.858×10^{-5}			

3 Peters Aerodynamic Model

Although Theodorsen's theory is an excellent choice in classical flutter analysis via the frequency domain, for the design of most controllers it is necessary to represent the actual aerodynamic loads in terms of differential

equations in the time domain and thus obtain a model of state space. In Peters method, the unsteady aerodynamic model is approximated in a finite dimensional state-space representation.

This model approximates the effects of unsteady air loads that form 2D incompressible flows using terms of induced flows to explain the effects of vortices on the flow near the airfoil. The wind speed near the airfoil is described by the free flow speed plus an additional local induced flow component as presented by Peters et al. [6]. In this theory the lift (L_a) and the pitch moment (M_a) are represented by:

$$L_a = \pi\rho_f b^2\left(\ddot{h} - b\overline{a}\ddot{\theta} + V_\infty\dot{\theta}\right) + 2\pi\rho_f bV_\infty\left[\dot{h} + b\Big(\frac{1}{2} - \overline{a}\Big)\dot{\theta} + V_\infty\theta - \vec{\lambda_0}\right] \tag{1}$$

$$M_a = \overline{a}bL + 2\pi\rho_f b^2\left[\frac{1}{2}V_\infty\dot{h} - \frac{1}{2}\overline{a}bV_\infty\dot{\theta} - \frac{1}{2}V_\infty\lambda_0 - \frac{1}{16}b^2\ddot{\theta}\right] \tag{2}$$

Where, $\overline{a}$ is the dimensionless elastic axis location, V_∞ the free flow speed, $\dot{h}$ and $\ddot{h}$ are the first and the second time derivatives of the deflection h of the structure in the domain of space and time and $\dot{\theta}$ and $\ddot{\theta}$ are the first and the second time derivatives of the elastic torsion deflection θ in the domain of space and time.

The lift (eq. 1) and moment (eq. 2) can be rewritten in a matricial form as:

$$\begin{bmatrix} -L_a \\ M_a \end{bmatrix} = [A]\begin{bmatrix} \ddot{h} \\ \ddot{\theta} \end{bmatrix} + [B]\begin{bmatrix} \dot{h} \\ \dot{\theta} \end{bmatrix} + [C]\begin{bmatrix} h \\ \theta \end{bmatrix} + [F]\vec{\lambda_0} \tag{3}$$

Where,

$$[A] = \begin{bmatrix} -L_{\ddot{h}} & -L_{\ddot{\theta}} \\ M_{\ddot{h}} & M_{\ddot{\theta}} \end{bmatrix}; \qquad [B] = \begin{bmatrix} -L_{\dot{h}} & -L_{\dot{\theta}} \\ M_{\dot{h}} & M_{\dot{\theta}} \end{bmatrix}; \qquad [C] = \begin{bmatrix} -L_h & -L_\theta \\ M_h & M_\theta \end{bmatrix}; \qquad [F] = \begin{bmatrix} -L_{\lambda 0} \\ M_{\lambda 0} \end{bmatrix} \tag{4}$$

With:

$$L_h = 0; \qquad L_{\dot{h}} = 2\pi\rho_f bV_\infty; \qquad L_{\ddot{h}} = \pi\rho_f b^2 \tag{5}$$

$$L_\theta = 2\pi\rho_f bV_\infty^2; \qquad L_{\dot{\theta}} = \pi\rho_f b^2V_\infty + 2\pi\rho_f b^2V_\infty\Big(\frac{1}{2} - \overline{a}\Big); \qquad L_{\ddot{\theta}} = -\pi\rho_f b^3\overline{a} \tag{6}$$

$$L_{\lambda_0} = -2\pi\rho_f bV_\infty; \qquad M_{\lambda_0} = -2\pi\rho_f b^2\overline{a}V_\infty - \pi\rho_f b^2V_\infty \tag{7}$$

$$M_h = 0; \qquad M_{\dot{h}} = 2\pi\rho_f b^2\overline{a}V_\infty + \pi\rho_f b^2V_\infty; \qquad M_{\ddot{h}} = \pi\rho_f b^3\overline{a} \tag{8}$$

$$M_\theta = 2\pi\rho_f b^2\overline{a}V_\infty^2; \quad M_{\dot{\theta}} = \pi\rho_f b^3\overline{a}V_\infty + 2\pi\rho_f b^3\overline{a}V_\infty\Big(\frac{1}{2} - \overline{a}\Big) - \pi\rho_f b^3\overline{a}V_\infty; \quad M_{\ddot{\theta}} = -\pi\rho_f b^4\overline{a}^2 - \frac{1}{8}\pi\rho_f b^4 \tag{9}$$

Equations 1 and 2 show that the lift contains circulatory and non-circulatory terms. The induced flow $\vec{\lambda_0}$ is expressed in terms of the airfoil movement, being approximated by a series of N states, given by:

$$\vec{\lambda_0}(t) = \frac{1}{2}\sum_{n=1}^{N}\vec{b_n}\lambda_n(t) \tag{10}$$

Since the coefficients of $\vec{b_n}$ are determined by the method of least squares, and given by:

$$\vec{b_n} = \begin{cases} (-1)^{n-1}\frac{(N+n)!}{(N-n)!}\frac{1}{(n!)^2} & \text{if } n \neq N \\ (-1)^{n-1} & \text{if } n = N \end{cases} \tag{11}$$

Equation 10 can be rewritten as:

$$\vec{\lambda_0} = [\tilde{b}]\vec{\lambda} \tag{12}$$

Where $\vec{\lambda}$ is a vector with a dimension of the number of states N. And, $[\tilde{b}]$ is a matrix resulting from the Kronecker product tensor with a dimension of the number of elements used in the discretization, so that:

$$[\tilde{b}] = \frac{1}{2}[I] \otimes \vec{b_n} \tag{13}$$

Given a column vector $\vec{\lambda}$ containing the values of λ_n, it is possible to write the set of N first-order ordinary differential equations for λ_n as:

$$[\tilde{A}]\dot{\vec{\lambda}} + \frac{V_\infty}{b}\vec{\lambda} = \vec{c_n}\left[\ddot{h} + V_\infty\dot{\theta} + b\Big(\frac{1}{2} - \overline{a}\Big)\ddot{\theta}\right] \tag{14}$$

Where the matrix $[\tilde{A}]$ and the vector $\vec{c_n}$ are composed of constants determined by the number of induced flow states, N. The matrix $[\tilde{A}]$ is given by:

$$[\tilde{A}] = [D_{nm}] + \vec{d_n}\vec{b_n}^T + \vec{c_n}\vec{d_n}^T + \frac{1}{2}\vec{c_n}\vec{b_n}^T \tag{15}$$

The matrix $[D_{nm}]$ and the vectors $\vec{c_n}$ and $\vec{d_n}$ can be obtained using:

$$[D_{nm}] = \begin{cases} \frac{1}{2n} & \text{if } n = m+1 \\ -\frac{1}{2n} & \text{if } n = m-1 \\ 0 & \text{if } n \neq m \pm 1 \end{cases} \qquad \vec{d_n} = \begin{cases} \frac{1}{2} & \text{if } n = 1 \\ 0 & \text{if } n \neq 1 \end{cases} \qquad \vec{c_n} = \frac{2}{n} \tag{16}$$

In this way, the eq. 14 can be rewritten as:

$$\dot{\vec{\lambda}} = [a_1]\vec{\lambda} + \vec{a_2}\ddot{h} + \vec{a_3}\dot{\theta} + \vec{a_4}\ddot{\theta} \tag{17}$$

Where,

$$[a_1] = [\tilde{A}]^{-1}\left(\frac{-V_\infty}{b}\right); \quad \vec{a_2} = [\tilde{A}]^{-1}\vec{c_n}; \quad \vec{a_3} = [\tilde{A}]^{-1}\vec{c_n}V_\infty; \quad \vec{a_4} = [\tilde{A}]^{-1}\vec{c_n}b\left(\frac{1}{2} - \overline{a}\right) \tag{18}$$

4 Aeroelastic Equations

In this section, the equations of motion are derived. Firstly, the kinetic and potential energy for the beam in torsion and bending is presented. Then, non-conservative forces are introduced in the expression of external work due to damping and aerodynamics. Finally, the equations are obtained from the Hamilton Principle.

The total kinetic energy of the system can be described as a function of elevation ($h(x,t)$) and pitch ($\theta(x,t)$) in the space and time domain along the length:

$$V_{h\theta} = \frac{1}{2}\int_0^L \begin{bmatrix} \dot{h}(x,t) \\ \dot{\theta}(x,t) \end{bmatrix}^T \begin{bmatrix} \rho ct + C\rho_p c_p t_p & S_{sc} \\ S_{sc} & \rho I + C\rho_p I_p \end{bmatrix} \begin{bmatrix} \dot{h}(x,t) \\ \dot{\theta}(x,t) \end{bmatrix} dx + \frac{1}{2}\begin{bmatrix} \dot{h}(x,t) \\ \dot{\theta}(x,t) \end{bmatrix}^T \begin{bmatrix} m & md \\ md & I_m \end{bmatrix} \begin{bmatrix} \dot{h}(x,t) \\ \dot{\theta}(x,t) \end{bmatrix} \Bigg|_L \tag{19}$$

Where, S_{sc} is static mass moment, $S_{sc} \neq 0$ in case the elastic axis is far from the center of gravity and C is a localizing function that describes the position of the piezoelectric patches:

$$C = \begin{cases} 0 & \text{if } x \leq p_1 \quad \text{or} \quad x \geq p_2 \\ 1 & \text{if } p_1 < x < p_2 \end{cases} \tag{20}$$

And the total potential energy of the system can be described as:

$$U_{h\theta} = \frac{1}{2}\int_0^L \begin{bmatrix} h''(x,t) \\ \theta''(x,t) \end{bmatrix}^T \begin{bmatrix} EI + CE_pI_p & 0 \\ 0 & 0 \end{bmatrix} \begin{bmatrix} h''(x,t) \\ \theta''(x,t) \end{bmatrix} dx + \frac{1}{2}\int_0^L \begin{bmatrix} h'(x,t) \\ \theta'(x,t) \end{bmatrix}^T \begin{bmatrix} 0 & 0 \\ 0 & GJ + CG_pJ_p \end{bmatrix} \begin{bmatrix} h'(x,t) \\ \theta'(x,t) \end{bmatrix} dx \tag{21}$$

So that I and I_p the moments of inertia of the beam and the piezoelectric element, respectively and GJ and G_pJ_p torsional beam and piezoelectric stiffness.

Since the damping occurs due to work related to non-conservative forces, it can be written in function of the structural damping (c_h) and structural damping of pitch (c_θ):

$$V_d = -\int_0^L \begin{bmatrix} h(x,t) \\ \theta(x,t) \end{bmatrix}^T \begin{bmatrix} c_h & 0 \\ 0 & c_\theta \end{bmatrix} \begin{bmatrix} \dot{h}(x,t) \\ \dot{\theta}(x,t) \end{bmatrix} dx \tag{22}$$

And the work of non-conservative forces related to aerodynamics:

$$W_{nc} = \int_0^L \begin{bmatrix} h(x,t) \\ \theta(x,t) \end{bmatrix}^T \left([A] \begin{bmatrix} \ddot{h}(x,t) \\ \ddot{\theta}(x,t) \end{bmatrix} + [B] \begin{bmatrix} \dot{h}(x,t) \\ \dot{\theta}(x,t) \end{bmatrix} + [C] \begin{bmatrix} h(x,t) \\ \theta(x,t) \end{bmatrix} + [F][\tilde{b}]\vec{\lambda} \right) dx \tag{23}$$

Where, the aerodynamic force varies as a function of x, and that it is calculated by the strip theory, i.e., a technique to solve a three-dimensional problem using known two-dimensional solutions in which the support surface is subdivided into strips arranged along the span. In other words, the flow along any section of the wing can be considered as two-dimensional.

Using the modal superposition principle, $h(x,t)$ and $\theta(x,t)$ can be expressed in terms of an enriched modal basis composed of m modes of bending and n modes of torsion:

$$\begin{bmatrix} h(x,t) \\ \theta(x,t) \end{bmatrix} = \begin{bmatrix} \vec{R}(x) & [0]_{1,m} \\ [0]_{1,n} & \vec{S}(x) \end{bmatrix} \begin{bmatrix} h(t) \\ \theta(t) \end{bmatrix} \tag{24}$$

Where, $\vec{R}(x)$ is the decoupled bending modes vector and $\vec{S}(x)$ the vector of decoupled twisting modes. Replacing the modal base (eq. 24) in the eq. 19 to 23:

$$V_{h\theta} = \frac{1}{2} \begin{bmatrix} \dot{h}(t) \\ \dot{\theta}(t) \end{bmatrix}^T [\mathbb{M}] \begin{bmatrix} \dot{h}(t) \\ \dot{\theta}(t) \end{bmatrix} \qquad U_{h\theta} = \frac{1}{2} \begin{bmatrix} h(t) \\ \theta(t) \end{bmatrix}^T [\mathbb{K}] \begin{bmatrix} h(t) \\ \theta(t) \end{bmatrix} \qquad V_d = - \begin{bmatrix} h(t) \\ \theta(t) \end{bmatrix}^T [\mathbb{D}] \begin{bmatrix} \dot{h}(t) \\ \dot{\theta}(t) \end{bmatrix} \tag{25}$$

$$W_{nc} = \begin{bmatrix} [h(t)] \\ [\theta(t)] \end{bmatrix}^T \left([\mathbb{A}] \begin{bmatrix} [\ddot{h}(t)] \\ [\ddot{\theta}(t)] \end{bmatrix} + [\mathbb{B}] \begin{bmatrix} [\dot{h}(t)] \\ [\dot{\theta}(t)] \end{bmatrix} + [\mathbb{C}] \begin{bmatrix} [h(t)] \\ [\theta(t)] \end{bmatrix} + [\mathbb{F}][\tilde{b}]\vec{\lambda} \right) \tag{26}$$

So that $[\mathbb{M}]$ is the mass matrix, $[\mathbb{K}]$ global stiffness matrix, $[\mathbb{D}]$ structural damping matrix, $[\mathbb{B}]$ aerodynamic stiffness matrix, $[\mathbb{C}]$ aerodynamic damping matrix, $[\mathbb{A}]$ the Peters matrix and $[\mathbb{F}]$ the induced flow matrix.

The aeroelastic model based on the Hamiltonian Principle and the aerodynamic strip theory can be described as:

$$\delta \int_0^t (V_{h\theta} - U_{h\theta})\, dt + \delta \int_0^t W_{nc}\, dt + \delta \int_0^t V_d\, dt = 0 \tag{27}$$

Replacing the previously obtained relations in eq. 27:

$$\delta \int_0^t \left(- \vec{q}^T[\mathbb{M}]\ddot{\vec{q}} - \vec{q}^T[\mathbb{K}]\vec{q} - \vec{q}^T[\mathbb{D}]\dot{\vec{q}} + \vec{q}^T[\mathbb{A}]\ddot{\vec{q}} + \vec{q}^T[\mathbb{B}]\dot{\vec{q}} + \vec{q}^T[\mathbb{C}]\vec{q} + \vec{q}^T[\mathbb{F}][\tilde{b}]\vec{\lambda} \right) dt = \vec{0} \tag{28}$$

Where,

$$\vec{q} = \begin{bmatrix} h(t) & \theta(t) \end{bmatrix}^T \tag{29}$$

Solving the eq. 28:

$$- [\mathbb{M}]\ddot{\vec{q}} - [\mathbb{K}]\vec{q} - [\mathbb{D}]\dot{\vec{q}} + [\mathbb{A}]\ddot{\vec{q}} + [\mathbb{B}]\dot{\vec{q}} + [\mathbb{C}]\vec{q} + [\mathbb{F}][\tilde{b}]\vec{\lambda} = \vec{0} \tag{30}$$

From there, the relationship can be established:

$$[T_1] \begin{bmatrix} \dot{\vec{q}} & \ddot{\vec{q}} & \dot{\vec{\lambda}} \end{bmatrix}^T = [T_2] \begin{bmatrix} \vec{q} & \dot{\vec{q}} & \vec{\lambda} \end{bmatrix}^T \tag{31}$$

Finally, the representative matrix of the complete system is obtained: $[Q] = [T_1]^{-1}[T_2]$. In compact way:

$$\dot{\vec{x}} - [Q]\vec{x} = \vec{0} \tag{32}$$

The eigenvalues of $[Q]$ can be used to study the stability of the aeroelastic system.

5 Aproximate Methods

For the analysis of vibration frequencies, flutter velocity and system behavior with piezoelectric control two approximate methods are used from routines created in the MATLAB environment: Finite Element Method and Rayleigh-Ritz with hierarchical standard and Bardell polynomials.

The Finite Element Method is used to determine the approximate solutions of bending and twisting frequencies and modes of vibration of the structure studied from the boundary conditions and their differential equations. In the process, the domain of the problem is divided into 50 elements of length (dx) and its accuracy is established. The method is widely discussed in the literature by Reddy [7].

The Rayleigh-Ritz with hierarchical Bardell polynomials porposed by Bardell [8] is a method in which the shape functions to satisfy the essential boundary conditions are based on hierarchical polynomial functions, as the recursive function defined as follows:

$$N_i = \sum_{r=0}^{j/2} \frac{(-1)^r (2j-2r-7)!!}{2^r r!(j-2r-1)!} \left[\frac{2x}{L} - 1\right]^{(j-2r-1)} , \quad j > 4 \tag{33}$$

Ten terms were used in the simulations that will be replaced in $\vec{R}$ and $\vec{S}$. The polynomials must have zero value in the root of the beam due to the clamped edge and consequent of bending and zero rotation, it must be assumed that the first two polynomials are neglected, since they have values different from 0 in the root.

Lastly, for the Rayleigh-Ritz with hierarchical standard polynomials, the following functions were simulated with ten terms:

$$N_i = \left[\frac{x}{L}\right]^{i+1} \tag{34}$$

6 Results and Discussion

This section shows the results obtained by Finite Element Method and by Rayleigh-Ritz (RR) via Bardell and standard hierarchical polynomials for the clamped beam with tip mass and coupled piezoelectric element treated as the model of this study. The Fig. 2 shows the four first modes of vibration of the beam subjected to bending and twisting, depending on their length.

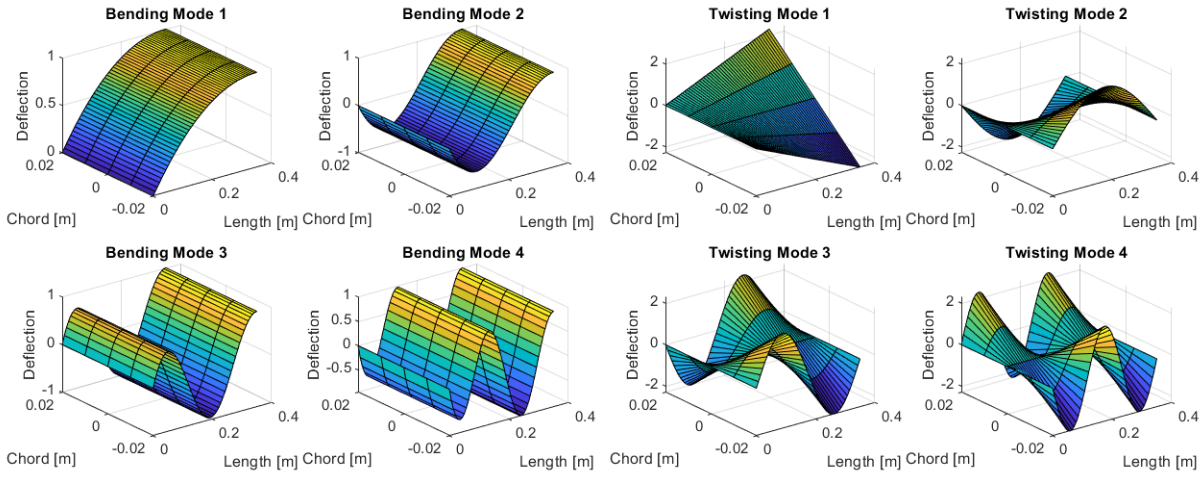

Figure 2. Four first bending and twisting modes for the model.

The results for the first four modes of vibration related to bending and torsion are shown in Table 2. It is important to note that, of the four modes, only the third is a contribution from torsion, the others are related to bending. It can be seen that the methods inspired by Rayleigh-Ritz have very close values and that their results converge to the frequencies obtained via Finite Elements, however with less computational cost.

Table 2. Vibration frequencies for the model subject to bending and torsion

Mode	Finite Elements [Hz]	RR Bardell [Hz]	RR Standard [Hz]
1st bending mode	2.3548	2.3545	2.3545
2nd bending mode	25.664	25.313	25.361
1st twisting mode	27.242	27.289	27.539
3rd bending mode	80.640	80.699	80.722

As a validation of the code developed in MATLAB, a simulation was performed for Goland wing, whose flutter speeds are easily found in the work of Haddadpour and Firouz-Abadi [9]. The flutter velocities for the

two wing models using Peters' unsteady aerodynamics using Rayleigh-Ritz methods with Bardell and Standard hierarchical polynomials can be seen in Table 3. Checking the results obtained for the Goland wing and comparing them with those found in the literature, it is concluded that the values obtained are close and the code developed can be validated. It is also possible to verify through the results obtained for Goland's wing that Peters' aerodynamic method is very accurate in comparison with the exact values found in the literature.

Finally, the results converge, with respect to the approach used for discretization (Finite Elements, Rayleigh-Ritz with standard and Bardell hierarchical polynomials).

Table 3. Wing Flutter Frequencies and Speeds

Goland	RR Bardell	RR Standard	Finite Elements	Bibliography [9]
Frequency [Hz]	71.22	71.83	71.19	71
Velocity [m/s]	137.28	137.49	137.22	137.46
Model	RR Bardell	RR Standard	Finite Elements	Bibliography [9]
Frequency [Hz]	27.02	27.20	27.03	-
Velocity [m/s]	10.0	10.0	10.0	-

7 Conclusions

In this work, a Rayleigh-Ritz-inspired method with Bardell hierarchical polynomials was used, leading to good accuracy and low computational cost. Together with this observation, we can conclude that Peters' non-stationary method presented good accuracy and the aeroelastic model was validated against literature results. The final semi-analytic models obtained in this work are appropriate for control design, since they lead to low order state-space models. Further work should explore the model obtained here for designing flutter suppression controllers with the use of the piezoelectric element.

Acknowledgements. This work was carried out with the support of the Coordination of Improvement of Higher Education Personnel - Brazil (CAPES).

Authorship statement. The authors hereby confirm that they are the sole liable persons responsible for the authorship of this work, and that all material that has been herein included as part of the present paper is either the property (and authorship) of the authors, or has the permission of the owners to be included here.

References

[1] Wright, J. R. & Cooper, J. E., 2007. *Introduction to Aircraft Aeroelasticity and Loads*. John Wiley and Sons Ltd.

[2] Dowell, E. H., Curtiss, Jr, H. C., & Scanlan, R. H., S., 1980. *A Modern Course in Aeroelasticity*. Alphen aan den Rijn, Sijtho and Noordho.

[3] Hodges, D. H. & Pierce, G. A., 2011. *Introduction to Structural Dynamics and Aeroelasticity*. Cambridge University Press.

[4] Franco, T. C., 2020. Modelagem e controle aeroelastico baseado em energia utilizando materiais piezoelétricos. Master's thesis, Instituto Tecnológico de Aeronáutica (ITA), São José dos Campos, Brazil.

[5] Franco, T. C. & Cardoso-Ribeiro, F. L., 2019. Modeling and energy-based control of a flexible wing with piezoelectric actuators. *Proceedings COBEM 2019*, vol. 25.

[6] Peters, D., Karunamoorthy, S., & Cao, W., 1995. Finite state induced flow models: Two-dimensional thin airfoil. *Journal of Aircraft*, vol. 32, pp. 313–322.

[7] Reddy, J., 2005. *An Introduction to the Finite Element Method*. 3rd Edition. McGraw-Hill Education (ISE Editions).

[8] Bardell, N., 1991. Free vibration analysis of a at plate using the hierarchical finite element method. *Journal of Sound and Vibration*, vol. 151, pp. 263–289.

[9] Haddadpour, H. & Firouz-Abadi, R., 2006. Evaluation of quasi-steady aerodynamic modeling for flutter prediction in subsonic flow. *Journal of Thin-Walled Structures*, vol. 44, pp. 931–936.